Neurochemistry International 58 (2011) 153–160

Contents lists available at ScienceDirect

Neurochemistry International

journal homepage: www.elsevier.com/locate/neuint

Anti-inflammatory activity of xanthohumol involves heme oxygenase-1 induction via NRF2-ARE signaling in microglial BV2 cells

Ik-Soo Lee [1], Juhee Lim [1], Jiyeong Gal, Jeen Chu Kang, Hyun Jung Kim, Bok Yun Kang, Hyun Jin Choi *

College of Pharmacy and Research Institute of Drug Development, Chonnam National University, 300 Yongbong-dong, Buk-gu, Gwangju 500-757, South Korea

ARTICLE INFO

Article history:
Received 27 May 2010
Received in revised form 25 October 2010
Accepted 10 November 2010
Available online 18 November 2010

Keywords:
Anti-inflammation
BV2
Heme oxigenase-1
Microglia
Nrf2
Xanthohumol

ABSTRACT

Xanthohumol (2′,4′,4-trihydroxy-6′-methoxy-3′-prenylchalcone) is a major chalcone derivative isolated from hop (*Humulus lupulus* L.) commonly used in brewing due to its bitter flavors. Xanthohumol has anti-carcinogenic, free radical-scavenging, and anti-inflammatory activities, but its precise mechanisms are not clarified yet. The basic leucine zipper (bZIP) protein NRF2 is a key transcription factor mediating the antioxidant and anti-inflammatory responses in animals. Therefore, we tested whether xanthohumol exerts anti-inflammatory activity in mouse microglial BV2 cells via NRF2 signaling. Xanthohumol significantly inhibited the excessive production of inflammatory mediators NO, IL-1β, and TNF-α, and the activation of NF-κB signaling in LPS-induced stimulated BV2 cells. Xanthohumol up-regulated the transcription of NAD(P)H:quinone oxidoreductase 1 (NQO1) and heme oxygenase-1 (HO-1), and increased the level of the endogenous antioxidant GSH. In addition, xanthohumol induced nuclear translocation of NRF2 and further activation of ARE promoter-related transcription. The anti-inflammatory response of xanthohumol was attenuated by transfection with NRF2 siRNA and in the presence of the HO-1 inhibitor, ZnPP, but not the NQO1 inhibitor, dicoumarol. Taken together, our study suggests that xanthohumol exerts anti-inflammatory activity through NRF2-ARE signaling and up-regulation of downstream HO-1, and could be an attractive candidate for the regulation of inflammatory responses in the brain.

1. Introduction

Inflammatory responses are a host defense mechanism, but can also play a crucial role in the underlying pathogenesis of inflammation-related disorders. Chronic neuroinflammation is a hallmark of neurodegenerative diseases, including Parkinson's disease (PD) (Wilms et al., 2007). Data from post-mortem studies indicate neuroinflammatory responses in PD; particularly the presence of activated microglial cells in the substantia nigra (McGeer et al., 1988), an increase in the levels of pro-inflammatory cytokines in the striatum and substantia nigra (Hunot et al., 1999; Reale et al., 2009), and activation of the pro-inflammatory NF-κB signaling, which regulates target genes encoding pro-inflammatory cytokines, chemokines, growth factors, and inducible enzymes (Mogi et al., 2007).

Microglia are resident immune cells in the central nervous system that respond to extracellular stimuli and play a crucial role in the progress of neuroinflammation (Sugama, 2009). Activated microglia can induce and release pro-inflammatory cytokines such as tumor necrosis factor (TNF)-α, interleukins (ILs)-1β, -6, and -2, as well as reactive oxygen and nitrogen species (Reale et al., 2009), which lead to inflammation-mediated neuronal cell death. Therefore, control of microglial activation may alleviate the progression of neurodegeneration, suggesting that development of anti-inflammatory drugs could provide a potential therapeutic approach for neurodegenerative conditions.

In this regard, increasing the intrinsic anti-inflammatory potency could be an especially desirable strategy to prevent inflammation-related neuronal injuries. There is a continuous interest in the anti-inflammatory effects of natural products, especially compounds present in foods that have been used in diet. Xanthohumol (XN), a major prenylated chalcone isolated from the hop plant *Humulus lupulus* L. (Cannabaceae), displays a wide range of biological activities; XN has chemopreventive effects on many cancer cell lines, and anti-angiogenic effects on human breast cancer MCF7 cells (Monteiro et al., 2008). The chemopreventive mechanism of XN occurs through induction of the detoxification enzyme NAD(P)H:quinone oxidoreductase-1 (NQO1) (Dietz et al., 2005). XN also has immunomodulatory activity in macrophage cell lines (Cho et al., 2008; Turchini et al., 2009), but the specific mechanisms of anti-inflammatory action have yet to be identified.

The transcription factor NF-E2-related factor 2 (NRF2) is a central protein that regulates the transcription of antioxidant

* Corresponding author. Tel.: +82 62 530 2938; fax: +82 62 530 2911.
E-mail address: hjchoi3@chonnam.ac.kr (H.J. Choi).
[1] These authors made equal contributions.

0197-0186/$ – see front matter © 2010 Elsevier Ltd. All rights reserved.
doi:10.1016/j.neuint.2010.11.008

proteins (Johnson et al., 2008). Under physiological conditions, NRF2 is sequestered in the cytoplasm by binding to Kelch-like ECH-associated protein 1 (Keap1). When stimulated, NRF2 dissociates from Keap1, and is translocated into the nucleus where it binds to antioxidant responsive element (ARE) and induces the expression of ARE-dependent genes (Johnson et al., 2008). ARE is a cis-acting regulatory element in promoter regions of genes encoding antioxidant proteins, and plays a crucial role in transcriptional regulation of downstream genes important in the cellular response to oxidative stress, such as NQO1 (Nioi and Hayes, 2004), heme oxygenase-1 (HO-1) (Martin et al., 2004), glutamate cysteine ligase (Okouchi et al., 2006), and glutathione S-transferase (Omata et al., 2008). In addition to the role of NRF2 signaling as a guardian of redox homeostasis, recent evidences have suggested the relevance in the immunomodulation of macrophages (Kapturczak et al., 2004). Exposure of NRF2-deficient mice to endotoxin leads to increased expression of pro-inflammatory cytokines compared to wild-type animals (Thimmulappa et al., 2006), and NRF2 activation suppresses lipopolysaccharide (LPS)-induced inflammation in mouse peritoneal macrophages (Lin et al., 2008).

In the present study, we asked (1) whether XN has anti-inflammatory activity against LPS-induced inflammatory responses in microglial BV2 cells, a murine microglial cell line that exhibits both phenotypic and functional properties of reactive microglial cells (Bocchini et al., 1992), (2) whether XN activates NRF2 signaling and increases downstream ARE-responsive proteins, and (3) whether XN-induced activation of NRF2 signaling could be a major cellular mechanism mediating anti-inflammatory effect of XN.

2. Materials and methods

2.1. Materials

XN was isolated and purified from hop pellets, which were obtained from Hopsteiner in Germany, as described by Stevens et al. (1997). Dulbecco's modified Eagle's medium (DMEM), fetal bovine serum (FBS), penicillin/streptomycin, and trypsin/EDTA were purchased from Hyclone (Logan, UT). LPS, dicoumarol, and ZnPP were from Sigma–Aldrich (St. Louis, MO). The antibody against β-actin was obtained from Cell Signaling Technology (Beverly, MA), and NRF2, NF-κB p65, and Lamin B antibodies were from Santa Cruz Biotechnology (Santa Cruz, CA). The enhanced Chemiluminescence (ECL) kit was obtained from Millipore (Piscataway, NJ). Texas red-X goat anti-rabbit IgG was purchased from Molecular Probes (Eugene, OR). Maxim RT-premix kit and Maxim PCR pre Mix kit were purchased from iNtRON (Seongnam, South Korea), and PCR primer was purchased from Bioneer (Daejon, South Korea). The GSH-400 kit was obtained from Bioxytech (OXIS International, Portland, USA). The NF-κB and pGL-ARE-reporter construct were from Kang KW (Chosun University, South Korea), and the dual-luciferase reporter assay system was purchased from Promega. All other chemicals were reagent grade and were purchased from Sigma–Aldrich or Merck (Rahway, NJ).

2.2. Cell culture

BV2 cells were obtained from ATCC (Manassas, VA) and maintained in DMEM containing 10% FBS, 100 U/ml penicillin/streptomycin at 37 °C in 5% CO_2 in a humidified atmosphere. Cells were plated on polystyrene culture dishes at 1.0×10^5 cells/well in 24-well culture plates or 1.1×10^6 cells/60 mm plates. After 24 h incubation, cells were fed with fresh medium for treatment.

2.3. Reverse transcription-polymerase chain reaction (RT-PCR)

Total RNA from cells were extracted using Tri-reagent (Molecular Research Center, Inc., Cincinnati, OH) according to the manufacturer's protocol. RT-PCR was performed using Maxim RT-premix kit and Maxim PCR pre Mix kit (iNtRON, Seongnam, South Korea) and primers. Primer sequences are shown in Table 1. PCR was performed at 94 °C for 30 s, 60 °C for 40 s, and 72 °C for 1 min for 30 cycles. PCR products were separated by 1.2% agarose gel electrophoresis. Gels were stained with ethidium bromide and analyzed under ultraviolet light.

2.4. NO assay

BV2 cells were plated at 1.0×10^5 cells/well in 24-well culture plates. After treatment with LPS in the presence or absence of XN, the amount of NO released in the culture media was measured using the method previously described (Lin et al., 2008).

2.5. Reduced glutathione (GSH) assay

GSH content was determined using the Bioxytech GSH-400 kit (OXIS International, Portland, OR) based on the manufacturer's protocol.

2.6. Transient transfection and luciferase assay

Cells were transfected with pNF-κB/or pGL-ARE and pRL-TK reporter plasmids using Hilymax according to the manufacturer's protocol (Dojindo Laboratories, Kumamoto, Japan). A dual-luciferase reporter assay system (Promega, WI) was used to determine NF-κB and ARE-driven promoter activity. Cells were plated at 0.5×10^5 cells/well in 24-well culture plates, and transiently transfected with pGL-ARE minimal reporter (a triplicate repeat of the ARE region of quinine oxidoreductase promoter)/or NF-κB luciferase and pRL-TK plasmid on the following day. After treatment with XN and LPS, firefly and Renilla luciferase activities in the cell lysates were determined using a luminometer (Microlumat Plus LB 96V, BERTHOLD).

2.7. NRF2 knockdown by siRNA transfection

BV2 cells were transfected with NRF2 siRNA using siRNA transfection reagent according to the manufacturer's protocol (Santa Cruz, CA).

2.8. Isolation of nuclear extract

The isolation of the nuclear fraction was performed based on the method of (Cho et al., 2008), with some modifications. Briefly, cells grown on 100 mm culture dishes were washed with ice-cold phosphate buffered saline (PBS), harvested, and centrifuged at $3000 \times g$ for 10 min at 4 °C. The pellet was obtained and resuspended in hypotonic buffer containing 10 mM HEPES (pH 7.9), 1.5 mM $MgCl_2$, 0.5 mM KCl, 0.5 mM DTT, and 0.2 mM phenylmethylsulfonyl fluoride. The lysates obtained were incubated for 10 min on ice with NP-40 and centrifuged at $14{,}000 \times g$ for 15 min at 4 °C. The supernatant, consisting of the cytosolic fraction, was immediately frozen for further analysis. The pellet was resuspended in low salt buffer containing 20 mM HEPES (pH 7.9), 1.5 mM $MgCl_2$, 25% glycerol, 0.02 mM KCl, 0.2 mM EDTA, 0.5 mM DTT, and 0.2 mM phenylmethylsulfonyl fluoride, and then tapped 20–30 times. Next, high salt buffer [20 mM HEPES (pH 7.9), 1.5 mM $MgCl_2$, 25% glycerol, 0.8 M KCl, 0.2 mM EDTA, 0.5 mM DTT, and 0.2 mM phenylmethylsulfonyl fluoride] was added and incubated for 20 min on ice. Samples were gently mixed for 30 min at 4 °C. After centrifugation at $14{,}000 \times g$ for 30 min, the supernatants containing nuclear extracts were obtained. Protein concentration was determined using Bradford reagent (Bio-Rad; Hercules, CA).

2.9. Western blotting

For immunoblot analysis, cells were washed with PBS, harvested, and lysed with RIPA buffer (50 mM Tris–Cl, pH 7.5, 150 mM NaCl, 1% NP-40, 0.5% DOC and 0.1% SDS). Equal amounts of proteins were separated on a 10% SDS polyacrylamide gel and transblotted onto polyvinylidene difluoride-nitrocellulose filters. Membranes were incubated with appropriate primary antibody anti-NRF2, anti-NF-κB p65, anti-iNOS, anti-COX-2, anti-β-actin, and anti-LaminB and then incubated with horseradish peroxide-conjugated secondary antibody. Specific bands were visualized using the enhanced Chemiluminescence (ECL) detection kit. The blots from the cytosolic and nuclear fraction were reprobed with anti-β-actin and anti-LaminB antibodies (1:5000) to serve as a control for gel loading.

Table 1
Primer sequences.

mRNA	Forward	Reverse
Mouse NQO1	5′ CTC GAG CTT TAG GGT CGT CTT G 3′	5′ AAG CTT CTG CAC CTT GCC CT 3′
Mouse HO-1	5′ CTA TGT AAA GCG TCT CCA 3′	5′ GTC TTT GTG TTC TCT GTC 3′
Mouse iNOS	5′ ATG TCC GAA GCA AAC ATC AC 3′	5′ TAA TGT CCA GGA AGT AGG TG 3′
Mouse IL-1β	5′ ATG GCA ACT GTT CCT GAA CTC AAC T 3′	5′ CAG GAC AGG TAT AGA TTC TTT CCT TT 3′
Mouse TNF-α	5′ CAG ACC CTC ACA CTC AGA TCA TCT T 3′	5′ CAG AGC AAT GAC TCC AAA GTA GAC CT 3′
Mouse actin	5′ CAT GTT TGA GAC CTT CAA CAC CCC 3′	5′ GCC ATC TCC TGC TCG AAG TCT AG 3′

2.10. Immunocytochemistry

BV2 cells were plated on poly-D-lysine-coated cover slips in 12-well culture plates. After XN treatment, cells were washed twice with PBS and fixed in cold 4% paraformaldehyde and 4% sucrose in PBS, pH 7.4, for 10 min. After washing twice in 1% BSA in PBS, the cells were permeabilized and blocked by treatment with 0.3% Triton X-100, 2% BSA, and 10% normal rabbit serum in PBS for 1 h at room temperature. The cells were incubated with anti-NRF2 (1:100; Santa Cruz) or anti-NF-κB p65 (1:200; Santa Cruz) in PBS containing 1% bovine serum albumin overnight. After washing twice with 1% BSA in PBS, the cells were incubated with Texas red-X goat anti-rabbit IgG (Molecular Probes, Eugene, OR) at room temperature for 1 h. After washing twice with 1% BSA in PBS, Hoechst staining was performed. Cell images were obtained by confocal microscopy.

2.11. Data analysis

Data were analyzed and expressed as mean ± S.E.M. Comparisons were made using ANOVA and Student's t test. $P < 0.05$ was considered statistically significant.

3. Results

3.1. XN inhibits LPS-induced inflammatory responses in mouse microglial BV2 cells

Microglia are resident immune-competent cells of the CNS and monitor immune insults and invading pathogens. To assess the role of XN in immunomodulation in the CNS, we first treated mouse microglial BV2 cells with 0.2 μg/ml LPS in the presence or absence of XN. As shown in Fig. 1, activation of microglial cells leads to the generation of NO, and induction of the inflammatory enzymes inducible NO synthase (iNOS) and cyclooxygenase-2 (COX-2) and inflammatory cytokines including IL-1β and TNF-α. We treated cells with 0.5–5 μg/ml XN, those concentration ranges of XN has no effects on BV2 cell viability (data not shown). When

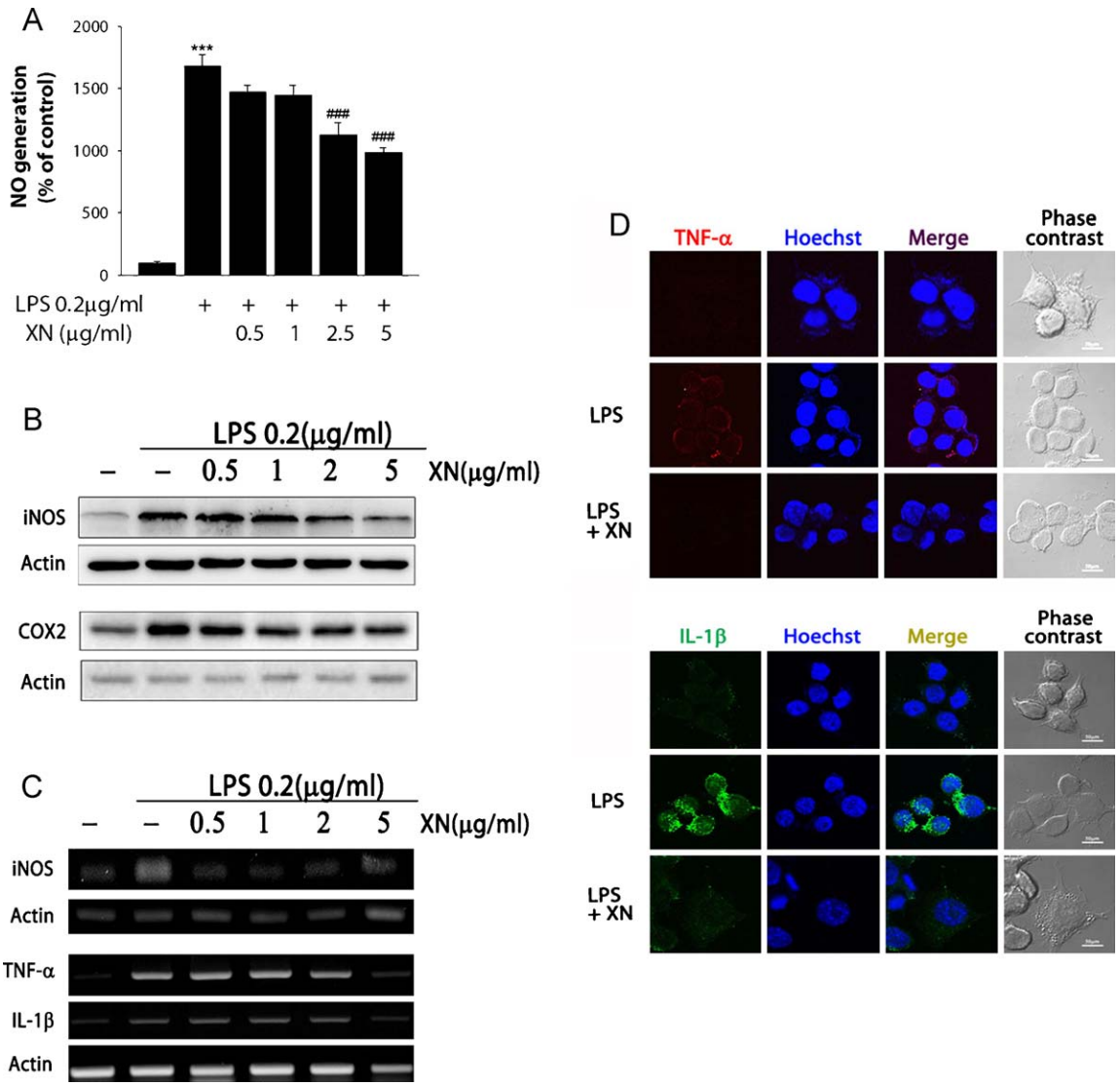

Fig. 1. Xanthohumol has anti-inflammatory activity against LPS-stimulated BV2 cells. (A) BV2 cells were pretreated with different concentrations of xanthohumol (0.5, 1, 2.5, or 5 μg/ml) for 1 h and subsequently co-treated with LPS (0.2 μg/ml) for additional 24 h. Released NO into the medium was measured using the Griess reagent. The results are expressed as the mean ± S.E.M. of percentage of untreated control obtained in four independent experiments; $^{***}P < 0.001$ versus untreated control, $^{\#\#\#}P < 0.001$ versus LPS only-treated group. (B) Cells were pretreated with different concentrations of xanthohumol for 1 h and subsequently co-treated with LPS (0.2 μg/ml) for additional 24 h. iNOS (upper panel) and COX-2 (lower panel) protein expression levels were monitored by Western blot analysis (loading control: β-actin). (C) BV2 cells were pretreated with xanthohumol for 1 h and subsequently co-treated with LPS for additional 3 h (for iNOS; upper panel) or 1 h (for TNF-α and IL-1β; lower panels), and iNOS and pro-inflammatory cytokines TNF-α and IL-1β mRNA levels were measured by RT-PCR. (D) Cells were pretreated with xanthohumol (5 μg/ml) for 1 h and subsequently co-treated with LPS for additional 24 h. The levels of TNF-α (upper panel) and IL-1β (lower panel) proteins in BV2 cells were analyzed by immunofluorescent confocal microscopic analysis (TNF-α, red fluorescence; IL-1β, green fluorescence). Hoechst staining (blue fluorescence) represents the nuclei. XN, xanthohumol. (For interpretation of the references to color in this figure legend, the reader is referred to the web version of the article.)

cells were pretreated with XN, LPS-induced accumulation of nitrite in the culture medium was significantly attenuated (Fig. 1A). Increase in nitrite levels was detected in LPS-treated cells (1678 ± 93% of untreated control cells), which was attenuated by the presence with XN (986 ± 36% of untreated control cells at 5 μg/ml). LPS-induced up-regulations of iNOS and COX-2 proteins were also significantly attenuated by pretreatment with XN (Fig. 1B). In addition, the mRNA levels of the inflammatory cytokines TNF-α and IL-1β were measured by RT-PCR analysis. The mRNA expression of TNF-α and IL-1β was increased in LPS-treated cells, which was completely blocked in 5 μg/ml XN-treated cells (Fig. 1C). To confirm the effects of XN on LPS-stimulated up-regulation of inflammatory cytokines, we detected protein expressions of TNF-α and IL-1β by immunocytochemistry in LPS-treated BV2 cells in the presence/or absence with XN. As shown in Fig. 1D, LPS increased immunofluorescence of TNF-α and IL-1β, and XN blocked these up-regulations (Fig. 1D). All these results suggest that XN attenuates LPS-induced inflammatory responses in microglial BV2 cells.

3.2. XN attenuates LPS-induced NF-κB activation

Activation of NF-κB signaling is central to the transcriptional regulation of inflammatory mediators induced by LPS (Adcock, 1997). And lots of studies have indicated that the anti-inflammatory effects of natural products, such as chalcone derivatives, are due to the inhibition of NF-κB activation (Hässig et al., 1999; Noonan et al., 2007). Therefore, we next asked whether XN inhibits LPS-induced NF-κB activation in BV2 cells. LPS induced nuclear translocation of NF-κB p65 (Fig. 2A) and increased the transcriptional activity of NF-κB (Fig. 2B). Pretreatment with XN (5 μg/ml) for 1 h significantly inhibited LPS-induced activation of NF-κB signaling; nuclear translocation (Fig. 2C and E) and transcriptional activation (Fig. 2D). These results indicate that XN negatively regulates LPS-induced NF-κB activation in BV2 cells.

3.3. XN induces NRF2 nuclear translocation and transcriptional activation

Several experiments have shown direct and indirect interaction of NRF2 and NF-κB signaling (Heiss et al., 2001; Liu et al., 2007). Because XN inhibited NF-κB activation in LPS-treated BV2 cells (Fig. 2) and many compounds triggering NRF2 signaling concomitantly repressed NF-κB signaling (Karuri et al., 2006), we asked whether XN has an effect on NRF2 signaling. NRF2 is in the cytosol under basal conditions. When activated, NRF2 is separated from Keap1 protein, translocated to the nucleus, and binds to a promoter region called the ARE, which is implicated in the regulation of downstream gene expression (Lee and Johnson, 2004). We therefore examined the effect of XN on intracellular localization of NRF2 in BV2 cells. Western blot analysis revealed that NRF2 was translocated into the nucleus by XN treatment, as early as 1 h post-treatment (Fig. 3A). Immunocytochemistry data (Fig. 3B) also showed that XN increased nuclear levels of NRF2 protein, indicating translocation from the cytoplasm into the nucleus. To determine whether XN activates ARE signaling, we performed reporter gene analysis using BV2 cells transfected with a mammalian expression vector pGL-797 containing the luciferase structural gene and ARE promoter region (Kang et al., 2003).

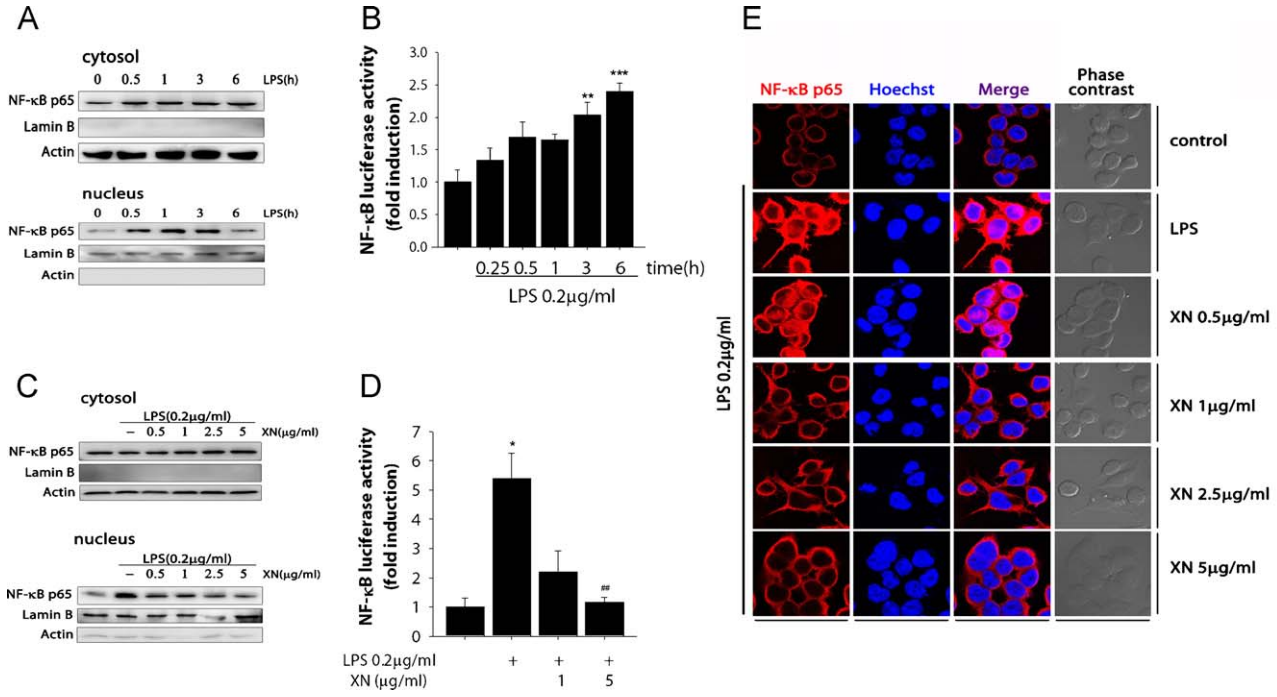

Fig. 2. Inhibitory effect of xanthohumol on LPS-induced NF-κB activation in BV2 cells. (A) BV2 cells were treated with 0.2 μg/ml LPS for the indicated durations (0, 0.5, 1, 3, or 6 h), and the levels of NF-κB p65 protein in the cytosol (upper panel) and nucleus (lower panel) were analyzed by Western blot analysis. (B) NF-κB transcriptional activity was determined by a reporter gene assay in LPS-treated and -untreated control cells. NF-κB luciferase activity was normalized to the Renilla luciferase activity in each sample. Data (mean ± S.E.M.) were representative of at least three independent experiments, and expressed as the fold-induction relative to untreated cells (at time zero). $^{**}P < 0.01$ and $^{***}P < 0.001$ versus untreated control. (C and E) Cells were pretreated with xanthohumol (0.5, 1, 2.5, or 5 μg/ml) for 1 h and subsequently co-treated with LPS (0.2 μg/ml) for additional 1 h. The effect of xanthohumol on the NF-κB nuclear translocation was determined by Western blotting analysis (C) and immunocytochemistry (E). The NF-κB p65 expression was normalized to the β-actin (cytosolic fraction) or Lamin B (nuclear fraction) level in each sample (C). Immunofluorescent confocal microscopy showed the level and location of NF-kB p65 (red fluorescence) in BV2 cells. Hoechst staining (blue fluorescence) represents the nuclei. (D) BV2 Cells were pretreated with xanthohumol (1 or 5 μg/ml) for 1 h, and the effect of xanthohumol on the LPS-induced NF-κB transcriptional activation was determined after 6 h of LPS treatment. The NF-κB luciferase activity was normalized to the Renilla luciferase activity in each sample. Data (mean ± S.E.M.) were representative of at least three independent experiments, and expressed as the fold-induction relative to untreated cells (at time zero); $^{*}P < 0.05$ versus untreated control; $^{\#\#}P < 0.01$ versus LPS alone-treated control. XN, xanthohumol. (For interpretation of the references to color in this figure legend, the reader is referred to the web version of the article.)

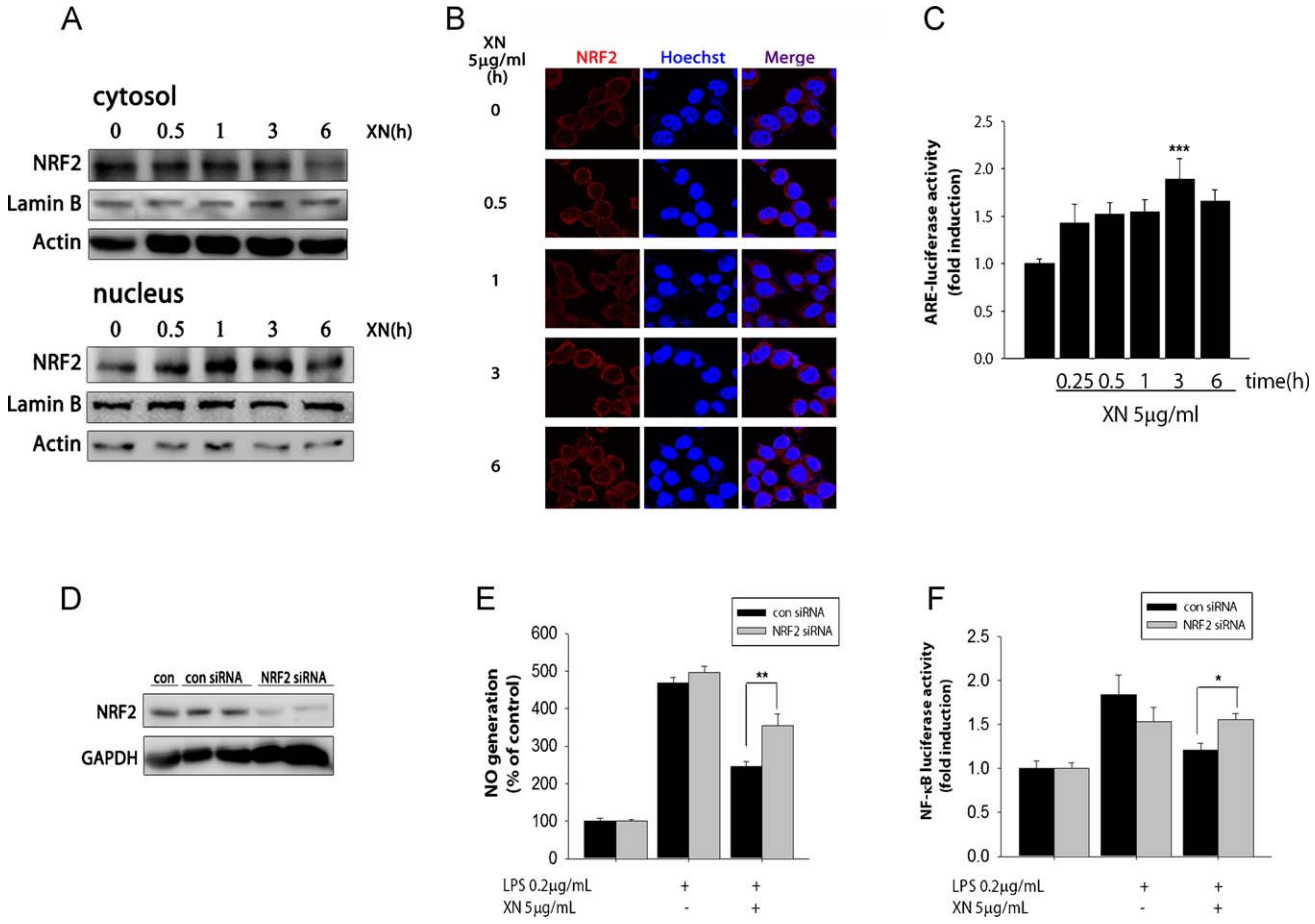

Fig. 3. NRF2-ARE signaling activation is involved in anti-inflammatory activity of xanthohumol. (A) BV2 cells were treated with 5 μg/ml xanthohumol for the indicated durations (0, 0.5, 1, 3, or 6 h), and the levels of NRF2 protein in cytosolic and nuclear fractions were analyzed by Western blot analysis. β-Actin and Lamin B were used as loading markers for cytosolic and nuclear fractions, respectively. (B) Immunofluorescent confocal microscopy showed the level and location of NRF2 (red fluorescence) in BV2 cells. Hoechest staining (blue fluorescence) represents the nuclei. (C) BV2 cells were treated with 5 μg/ml xanthohumol for the indicated durations (0, 0.25, 0.5, 1, 3, or 6 h), and ARE luciferase activity was measured. Cells were transiently transfected with the GSTA2 chimeric gene construct pGL-797 containing the ARE element or pGL-ARE minimal reporter, and dual luciferase reporter assay was performed on the lysed cells co-transfected with pGL-797/pGL-ARE (firefly luciferase) and pRL-TK (Renilla luciferase). ARE luciferase activity was normalized to the Renilla luciferase activity in each sample. Data (mean ± S.E.M.) were representative of at least three independent experiments, and expressed as the fold-induction relative to untreated cells (at time zero); $^{***}P < 0.001$ versus untreated control. (D) BV2 cells were transiently transfected with Nrf2 siRNA (100 pmol/6 well) for 24 h. Nrf2 protein levels were measured by Western blotting analysis with Nrf2 antibody. GAPDH was used as a loading control. (E and F) After Nrf2 siRNA transfection, BV2 cells were pretreated with XN for 1 h and subsequently co-treated with 0.2 μg/ml LPS for 24 h (E) and cells were transiently transfected with NF-kB luciferase plasmid and pRL-tK(F). Released NO in the medium was assessed using the Griess reagent. NO generation was expressed as mean ± S.E.M. as fold-induction of untreated control. $^{**}P < 0.01$ versus XN and LPS-treated normal control cells. (F) After transfection, cells were pretreated with XN for 1 h and subsequently co-treated with 0.2 μg/ml LPS for 6 h. The NF-κB luciferase activity was measured and normalized to the Renilla luciferase activity in each sample. Data (mean ± S.E.M.) were representative of at least three independent experiments, and expressed as the fold-induction relative to untreated cells (at time zero); $^{*}P < 0.05$ versus control siRNA-transfected cells treated with XN and LPS. XN, xanthohumol. (For interpretation of the references to color in this figure legend, the reader is referred to the web version of the article.)

Treatment with 5 μg/ml XN significantly increased ARE-luciferase activity in BV2 cells: 1.88 ± 0.21-fold increases after 3 h (Fig. 3C). These results suggest that XN activates the NRF2-ARE pathway.

Next, we asked whether XN-induced Nrf2 activation mediates anti-inflammatory responses of XN in LPS-treated BV2 cells. To confirm the contributions of NRF2 signaling to the suppressive effects of XN on LPS-induced inflammatory response, we transiently transfected cells with NRF2 siRNA and evaluated the effects of XN on LPS-induced NO generation and increase in NF-κB luciferase activity (Fig. 3D–F). As shown in Fig. 3D, transfection with NRF2 siRNA significantly inhibited the NRF2 protein expression in BV2 cells. XN-induced suppression of LPS-stimulated NO generation was attenuated by silencing NRF2 expression (Fig. 3E). Suppressive effect of XN on LPS-induced NF-κB activation was also reduced by silencing NRF2 expression (Fig. 3F). These data suggest a crucial role for the transcriptional activator NRF2 in the anti-inflammatory potential of XN.

3.4. XN induces ARE-driven NQO1 and HO-1 enzymes in BV2 cells

NRF2 is a transcription factor regulating expression of downstream antioxidant enzymes including NQO1 and HO-1, which are involved in the regulation of cellular antioxidant responses as well as acute inflammatory responses (Hsieh et al., 2006; Wu et al., 2006). Therefore, we asked whether XN increases gene expression of downstream antioxidant enzymes. XN increased both NQO1 and HO-1 mRNA levels (Fig. 4A) as well as protein levels (Fig. 4B). Maximum increases in mRNA and protein levels of NQO1 and HO-1 were detected after 3 h and 24 h of XN treatment, respectively. In addition, increased amount of reduced glutathione GSH was detected in XN-treated cells (Fig. 4C). All

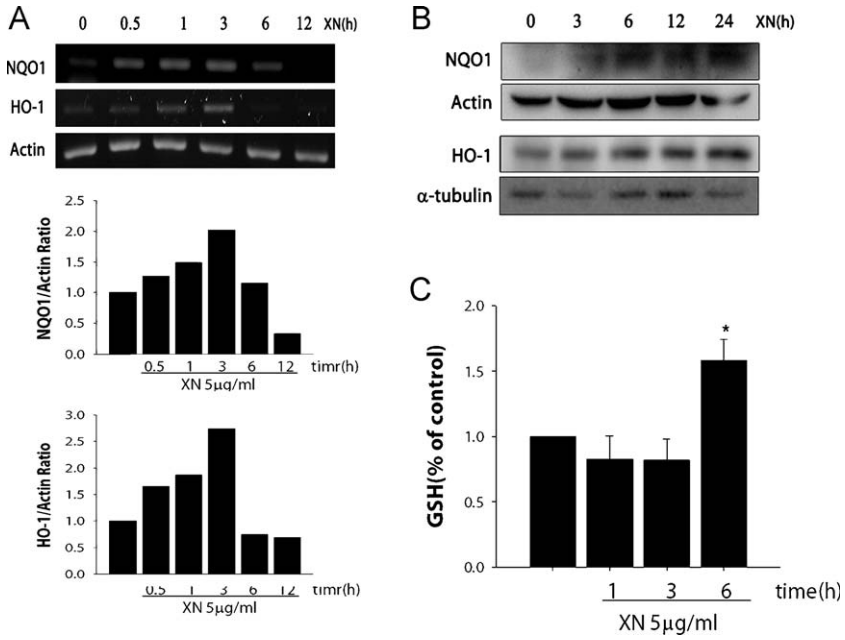

Fig. 4. Xanthohumol up-regulates ARE-downstream enzyme expression. (A) BV2 cells were treated with 5 μg/ml xanthohumol for the indicated durations (0.5, 1, 3, 6, or 12 h) and the mRNA levels of NQO1 (upper panel) and HO-1 (lower panel) were analyzed by RT-PCR. The results are represented as fold induction. (B) Cells were treated with 5 μg/ml xanthohumol for the indicated durations, and protein levels of NQO1 (upper panel) and HO-1 (lower panel) were analyzed by Western blotting. β-Actin and α-tubulin were used as loading controls, respectively. (C) GSH levels of xanthohumol-treated or -untreated cells were measured using the Bioxytech GSH-400 kit. Results are means ± S.E.M. $^{*}P < 0.05$ versus untreated control. XN, xanthohumol.

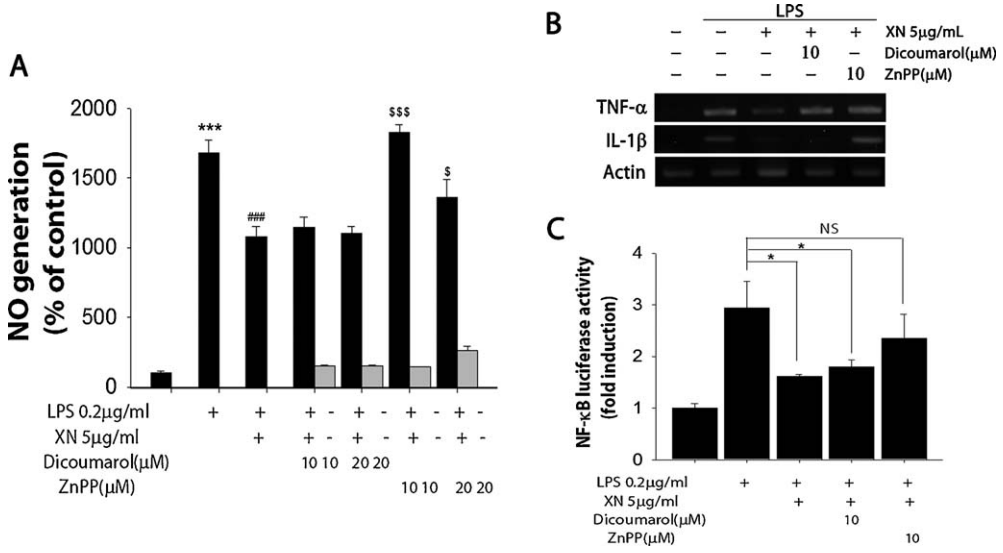

Fig. 5. Contribution of HO-1 induction to the anti-inflammatory effect of xanthohumol. (A) BV2 cells were exposed to 5 μg/ml xanthohumol for 1 h in the presence or absence with NQO1 inhibitor dicoumarol (10 and 20 μM) or HO-1 inhibitor ZnPP (10 and 20 μM), and were subsequently treated with 0.2 μg/ml LPS for additional 24 h. Degrees of NO production were expressed as mean ± S.E.M. in percentage of untreated control; $^{***}P < 0.001$ versus untreated control, $^{\#\#\#}P < 0.001$ versus LPS alone-treated control; $^{\$}P < 0.05$ and $^{\$\$\$}P < 0.001$ versus LPS and xanthohumol-treated cells. (B and C) Cells were treated with xanthohumol for 1 h in the presence or absence with dicoumarol (10 μM) or ZnPP (10 μM), and were subsequently treated with LPS for additional 1 h (B) or 6 h (C). (B) mRNA levels of TNFα and IL-1β were analyzed by RT-PCR. (C) The NF-κB luciferase activity was measured and normalized to the Renilla luciferase activity in each sample. Data (mean ± S.E.M.) were representative of at least three independent experiments, and expressed as the fold-induction relative to untreated cells (at time zero); $^{*}P < 0.05$ versus LPS-treated control cells. NS, not significant; XN, xanthohumol.

these data suggest XN up-regulates NRF2-ARE responsive enzymes.

3.5. XN exerts anti-inflammatory activity through induction of HO-1 in BV2 cells

To identify the NRF2 downstream enzymes which are mainly responsible for the anti-inflammatory activity of XN against LPS-induced inflammatory responses in BV2 cells, we first tested the effects of specific NQO1 inhibitor dicoumarol (Murphy et al., 1991) or HO-1 inhibitor zinc protoporphyrin IX (ZnPP) (Miyake et al., 2010) on anti-inflammatory effect of XN. As shown in Fig. 5A, ZnPP, but not dicoumarol, blocked the suppressive effect of XN on LPS-stimulated NO generation, suggesting that the anti-inflammatory effect of XN is primarily due to increased HO-1 activity. ZnPP also significantly abolished the inhibitory effects of XN on LPS-induced up-regulation of TNF-α and IL-1β mRNAs (Fig. 5B) as well as LPS-induced increase in NF-κB transcriptional activity (Fig. 5C). On the

other hand, dicoumarol blocked the XN-induced suppression of LPS responses in TNF-α mRNA levels only. Together, anti-inflammatory activity of XN seems to mainly involve the induction of HO-1.

4. Discussion

The present study demonstrates that (1) XN obtained from the hop plant *H. lupulus* L. inhibits LPS-stimulated inflammatory responses in microglial BV2 cells, (2) XN activates the NRF2 pathway and up-regulates the antioxidant enzymes, NQO1 and HO-1, and (3) the anti-inflammatory mechanism of XN requires induction of HO-1.

NRF2 is found in most cell types of the brain, including microglia, where it primarily regulates the expression of several antioxidant genes participating in redox homeostasis (Johnson et al., 2008). The innate immune response involves generation of reactive oxygen species (ROS), which can act as second messengers activating signaling pathways such as NF-κB (Roebuck, 1999). Recent evidences have indicated that ROS is generated in response to an inflammatory signal and participates in microglial activation (Fremond et al., 2007), and NRF2 could modulate brain redox homeostasis and regulate inflammatory conditions. Therefore, NRF2 signaling could be an attractive therapeutic target for brain inflammation; NRF2 knockout mice were more susceptible to the inflammatory response in the brain (Innamorato et al., 2008), sulforaphane-treated animals displayed NRF2 activation and increased in HO-1, with an attenuated production of inflammation markers after LPS treatment (Lin et al., 2008), and knockout of the NRF2 downstream enzyme, NQO1, increased the sensitivity to skin carcinogenesis (Iskander et al., 2005). In addition, aged mice were getting highly sensitive to oxidative stress with losing NRF2 activity, and NRF2-null mice are similar to aged animals (Duan et al., 2009). Loss of NRF2 signaling increases susceptibility to inflammation and 1-methyl-4-phenyl-1,2,3,6-tetrahydropyridine (MPTP)-induced toxicity (Yates et al., 2009).

Here, XN attenuated LPS-induced inflammatory responses such as NO release, up-regulation of iNOS, IL-1β, and TNF-α (Fig. 1), and NF-κB activation in microglial BV2 cells (Fig. 2). The involvement of NRF2 signaling in anti-inflammatory activity of XN is evidenced by the present findings showing that (1) XN induces NRF2 nuclear translocation, ARE-transcriptional activation (Fig. 3A–C), as well as up-regulation of its downstream enzymes NQO1 and HO-1 (Fig. 4), and (2) anti-inflammatory effects of XN are attenuated in NRF2-knockdown BV2 cells (Fig. 3D–F) and by the presence with specific inhibitor of HO-1 (Fig. 5A–C). Although we did not directly evaluate in the present study the mechanism how can XN activate NRF2 signaling in BV2 cells, it can be explained by the potential of XN to alkylate Keap1 protein (La et al., 2009). Alkylation of cysteine sulfhydryl groups of KEAP1 leads Keap1-NRF2 dissociation, and therefore induces NRF2 nuclear translocation and ARE-mediated up-regulation of cytoprotective gene expression (Zhou et al., 2003). Natural products containing electrophilic unsaturated ketones, including XN, are proposed to alkylate Keap1 protein (Luo et al., 2007). In particular, XN is reported to alkylate C151 residue of Keap1, which is essential for Keap1-NRF2 signaling system.

Among the downstream genes dependent on NRF2 activity, HO-1 induction represents an adaptive response that increases cellular resistance to inflammatory stimuli. HO-1 levels are very low under normal conditions, but can be up-regulated by a variety of stimuli, including oxidative stress, heat shock, ultraviolet radiation, cytokines, and its substrate heme (Kawakami et al., 2006; Shibahara, 1988) and play a crucial role in cytoprotection against inflammatory and oxidative damage. Current reports have suggested that activation of HO-1 inhibits NF-κB activation (Yeh et al., 2009) and attenuates the mRNA up-regulation of IL-10, TNF-α, and FasL (Ke et al., 2007). HO-1 induction also inhibits the production of pro-inflammatory cytokines including TNF-α in response to LPS (Lee and Chau, 2002; Otterbein et al., 2000). In the present study, XN increased both NQO1 and HO-1 mRNA expression (Fig. 3A–C), but only the HO-1 inhibitor, not the NQO1 inhibitor, attenuated all the suppressive effects of XN on LPS-stimulated increase; LPS-induced NO generation (Fig. 5A), up-regulation of TNF-α and IL-1β mRNAs (Fig. 5B), NF-κB activation (Fig. 5C). Although there have been reported that ZnPP could exert cellular effects independent of HO-1 activity (La et al., 2009), these data with our other data from NRF2 knockdown cells (Fig. 3D–F) support the major contribution of HO-1 in anti-inflammatory activity of XN, our present data. HO-1 catalyzes the degradation of heme to generate carbon monoxide, bilirubin, and free iron. The suggested immunomodulatory mechanism of HO-1 is as follows: (1) molecular oxygen is used during the enzyme reaction, attenuating oxidative stress (Cuadrado and Rojo, 2008), (2) carbon monoxide inhibits NADPH oxidase in LPS signaling (Li et al., 2008), and (3) bilirubin inhibits microglia activation (Min et al., 2006).

HO-1 expression in the brain has also been reported to be inducible by several chemicals including dietary-derived substances (Syapin, 2008). The plant diarylheptanoid derivative was reported to reduce iNOS expression in BV2 cells, accompanying with HO-1 up-regulation (Lee et al., 2005). Treatment with sulforaphane also protected neuronal cells from inflammation-related neurotoxicity through its capacity to modulate brain inflammation in animal models (Innamorato et al., 2008). Although we did not evaluate in the present study whether XN, a prominent flavonoid of the hop plant, can modulate neuroinflammatory processes and protect brain from inflammation-related neuronal damage *in vivo*, we showed for the first time that XN has anti-inflammatory activity in microglial cells. In general, the entry of drugs into the CNS is regulated by blood–brain barrier. Because this barrier can limit the entry of many chemicals that could induce HO-1 expression in the CNS and there is no information on the ability of XN to enter the CNS, relevance of anti-inflammatory activity of XN in the brain is not simple. But there are strong evidences showing that structurally different flavonoids are able to traverse the blood–brain barrier *in vivo* (Youdim et al., 2004). In addition, if CNS is damaged, they could more easily allow the entry of blood and various molecules that regulate cellular responses.

Due to beneficial biological activities of XN, growing attention has been focused on its application in humans as a medicine or diet. In the present study, XN did not exert cytotoxicity to BV2 cells in a concentration range of 0.5–5 μg/ml. Although we did not examine the efficacy and safety of XN in these concentrations in primary cultured microglial cells or in animal models, many *in vitro* biological activities of XN have been evaluated in these concentration ranges. In addition, previous toxicological studies in mice demonstrate that LD50 for oral dose of hop extract ranges from 500 to 3500 mg/kg (Zanoli and Zavatti, 2008), and oral administration of XN to mice did not affect major organ functions and metabolism (Vanhoecke et al., 2005).

In the present study, we observed that the prenylated chalcone XN inhibited inflammatory responses induced by LPS in microglial BV2 cells. We also demonstrated that these pharmacological effects of XN were associated with the NRF2-ARE pathway, especially HO-1 induction. The novel effect of XN on the regulation of NRF2 signaling and provides an attractive strategy to prevent neurodegenerative diseases associated with inflammation and attenuate the progress of the diseases.

Acknowledgement

This work was supported by the Korea Research Foundation Grant funded by the Korean Government (KRF-2008-220-E00042).

References

Adcock, I., 1997. Transcription factors as activators of gene transcription: AP-1 and NF-kappa B. Monaldi Arch. Chest Dis. 52, 178–186.

Bocchini, V., Mazzolla, R., Barluzzi, R., Blasi, E., Sick, P., Kettenmann, H., 1992. An immortalized cell line expresses properties of activated microglial cells. J. Neurosci. Res. 31, 616–621.

Cho, Y., Kim, H., Kim, Y., Lee, K., Choi, H., Lee, I., Kang, B., 2008. Differential anti-inflammatory pathway by xanthohumol in IFN-gamma and LPS-activated macrophages. Int. Immunopharmacol. 8, 567–573.

Cuadrado, A., Rojo, A., 2008. Heme oxygenase-1 as a therapeutic target in neurodegenerative diseases and brain infections. Curr. Pharm. Des. 14, 429–442.

Dietz, B., Kang, Y., Liu, G., Eggler, A., Yao, P., Chadwick, L., Pauli, G., Farnsworth, N., Mesecar, A., van Breemen, R., Bolton, J., 2005. Xanthohumol isolated from Humulus lupulus inhibits menadione-induced DNA damage through induction of quinone reductase. Chem. Res. Toxicol. 18, 1296–1305.

Duan, W., Zhang, R., Guo, Y., Jiang, Y., Huang, Y., Jiang, H., Li, C., 2009. Nrf2 activity is lost in the spinal cord and its astrocytes of aged mice. In Vitro Cell. Dev. Biol. Anim. 45, 388–397.

Fremond, C., Togbe, D., Doz, E., Rose, S., Vasseur, V., Maillet, I., Jacobs, M., Ryffel, B., Quesniaux, V., 2007. IL-1 receptor-mediated signal is an essential component of MyD88-dependent innate response to Mycobacterium tuberculosis infection. J. Immunol. 179, 1178–1189.

Hässig, A., Liang, W., Schwabl, H., Stampfli, K., 1999. Flavonoids and tannins: plant-based antioxidants with vitamin character. Med. Hypotheses 52, 479–481.

Heiss, E., Herhaus, C., Klimo, K., Bartsch, H., Gerhäuser, C., 2001. Nuclear factor kappa B is a molecular target for sulforaphane-mediated anti-inflammatory mechanisms. J. Biol. Chem. 276, 32008–32015.

Hsieh, T., Lu, X., Wang, Z., Wu, J., 2006. Induction of quinone reductase NQO1 by resveratrol in human K562 cells involves the antioxidant response element ARE and is accompanied by nuclear translocation of transcription factor Nrf2. Med. Chem. 2, 275–285.

Hunot, S., Dugas, N., Faucheux, B., Hartmann, A., Tardieu, M., Debré, P., Agid, Y., Dugas, B., Hirsch, E., 1999. FcepsilonRII/CD23 is expressed in Parkinson's disease and induces, in vitro, production of nitric oxide and tumor necrosis factor-alpha in glial cells. J. Neurosci. 19, 3440–3447.

Innamorato, N., Rojo, A., García-Yagüe, A., Yamamoto, M., de Ceballos, M., Cuadrado, A., 2008. The transcription factor Nrf2 is a therapeutic target against brain inflammation. J. Immunol. 181, 680–689.

Iskander, K., Gaikwad, A., Paquet, M., Long, D.n., Brayton, C., Barrios, R., Jaiswal, A., 2005. Lower induction of p53 and decreased apoptosis in NQO1-null mice lead to increased sensitivity to chemical-induced skin carcinogenesis. Cancer Res. 65, 2054–2058.

Johnson, J., Johnson, D., Kraft, A., Calkins, M., Jakel, R., Vargas, M., Chen, P., 2008. The Nrf2-ARE pathway: an indicator and modulator of oxidative stress in neurodegeneration. Ann. N. Y. Acad. Sci. 1147, 61–69.

Kang, K., Cho, I., Lee, C., Kim, S., 2003. Essential role of phosphatidylinositol 3-kinase-dependent CCAAT/enhancer binding protein beta activation in the induction of glutathione S-transferase by oltipraz. J. Natl. Cancer Inst. 95, 53–66.

Kapturczak, M., Wasserfall, C., Brusko, T., Campbell-Thompson, M., Ellis, T., Atkinson, M., Agarwal, A., 2004. Heme oxygenase-1 modulates early inflammatory responses: evidence from the heme oxygenase-1-deficient mouse. Am. J. Pathol. 165, 1045–1053.

Karuri, A., Huang, Y., Bodreddigari, S., Sutter, C., Roebuck, B., Kensler, T., Sutter, T., 2006. 3H-1,2-dithiole-3-thione targets nuclear factor kappaB to block expression of inducible nitric-oxide synthase, prevents hypotension, and improves survival in endotoxemic rats. J. Pharmacol. Exp. Ther. 317, 61–67.

Kawakami, T., Takahashi, T., Shimizu, H., Nakahira, K., Takeuchi, M., Katayama, H., Yokoyama, M., Morita, K., Akagi, R., Sassa, S., 2006. Highly liver-specific heme oxygenase-1 induction by interleukin-11 prevents carbon tetrachloride-induced hepatotoxicity. Int. J. Mol. Med. 18, 537–546.

Ke, B., Shen, X., Tsuchihashi, S., Gao, F., Araujo, J., Busuttil, R., Ritter, T., Kupiec-Weglinski, J., 2007. Viral interleukin-10 gene transfer prevents liver ischemia-reperfusion injury: toll-like receptor-4 and heme oxygenase-1 signaling in innate and adaptive immunity. Hum. Gene Ther. 18, 355–366.

La, P., Fernando, A., Wang, Z., Salahudeen, A., Yang, G., Lin, Q., Wright, C., Dennery, P., 2009. Zinc protoporphyrin regulates cyclin D1 expression independent of heme oxygenase inhibition. J. Biol. Chem. 284, 36302–36311.

Lee, T., Chau, L., 2002. Heme oxygenase-1 mediates the anti-inflammatory effect of interleukin-10 in mice. Nat. Med. 8, 240–246.

Lee, J., Johnson, J., 2004. An important role of Nrf2-ARE pathway in the cellular defense mechanism. J. Biochem. Mol. Biol. 37, 139–143.

Lee, C., Lee, S., Chen, S., Ho, F., Lin, W., 2005. Oregonin inhibits lipopolysaccharide-induced iNOS gene transcription and upregulates HO-1 expression in macrophages and microglia. Br. J. Pharmacol. 146, 378–388.

Li, X., Schwacha, M., Chaudry, I., Choudhry, M., 2008. Heme oxygenase-1 protects against neutrophil-mediated intestinal damage by down-regulation of neutrophil p47phox and p67phox activity and O2-production in a two-hit model of alcohol intoxication and burn injury. J. Immunol. 180, 6933–6940.

Lin, W., Wu, R., Wu, T., Khor, T., Wang, H., Kong, A., 2008. Sulforaphane suppressed LPS-induced inflammation in mouse peritoneal macrophages through Nrf2 dependent pathway. Biochem. Pharmacol. 76, 967–973.

Liu, Y., Hsieh, C., Wu, C., Wung, B., 2007. Chalcone inhibits the activation of NF-kappaB and STAT3 in endothelial cells via endogenous electrophile. Life Sci. 80, 1420–1430.

Luo, Y., Eggler, A., Liu, D., Liu, G., Mesecar, A., van Breemen, R., 2007. Sites of alkylation of human Keap1 by natural chemoprevention agents. J. Am. Soc. Mass Spectrom. 18, 2226–2232.

Martin, D., Rojo, A., Salinas, M., Diaz, R., Gallardo, G., Alam, J., De Galarreta, C., Cuadrado, A., 2004. Regulation of heme oxygenase-1 expression through the phosphatidylinositol 3-kinase/Akt pathway and the Nrf2 transcription factor in response to the antioxidant phytochemical carnosol. J. Biol. Chem. 279, 8919–8929.

McGeer, P., Itagaki, S., Boyes, B., McGeer, E., 1988. Reactive microglia are positive for HLA-DR in the substantia nigra of Parkinson's and Alzheimer's disease brains. Neurology 38, 1285–1291.

Min, K., Yang, M., Kim, S., Jou, I., Joe, E., 2006. Astrocytes induce hemeoxygenase-1 expression in microglia: a feasible mechanism for preventing excessive brain inflammation. J. Neurosci. 26, 1880–1887.

Miyake, M., Fujimoto, K., Anai, S., Ohnishi, S., Nakai, Y., Inoue, T., Matsumura, Y., Tomioka, A., Ikeda, T., Okajima, E., Tanaka, N., Hirao, Y., 2010. Inhibition of heme oxygenase-1 enhances the cytotoxic effect of gemcitabine in urothelial cancer cells. Anticancer Res. 30, 2145–2152.

Mogi, M., Kondo, T., Mizuno, Y., Nagatsu, T., 2007. p53 protein, interferon-gamma, and NF-kappaB levels are elevated in the parkinsonian brain. Neurosci. Lett. 414, 94–97.

Monteiro, R., Calhau, C., Silva, A., Pinheiro-Silva, S., Guerreiro, S., Gärtner, F., Azevedo, I., Soares, R., 2008. Xanthohumol inhibits inflammatory factor production and angiogenesis in breast cancer xenografts. J. Cell. Biochem. 104, 1699–1707.

Murphy, T., De Long, M., Coyle, J., 1991. Enhanced NAD(P)H:quinone reductase activity prevents glutamate toxicity produced by oxidative stress. J. Neurochem. 56, 990–995.

Nioi, P., Hayes, J., 2004. Contribution of NAD(P)H:quinone oxidoreductase 1 to protection against carcinogenesis, and regulation of its gene by the Nrf2 basic-region leucine zipper and the arylhydrocarbon receptor basic helix-loop-helix transcription factors. Mutat. Res. 555, 149–171.

Noonan, D., Benelli, R., Albini, A., 2007. Angiogenesis and cancer prevention: a vision. Recent Results Cancer Res. 174, 219–224.

Okouchi, M., Okayama, N., Alexander, J., Aw, T., 2006. NRF2- dependent glutamate-L-cysteine ligase catalytic subunit expression mediates insulin protection against hyperglycemia-induced brain endothelial cell apoptosis. Curr. Neurovasc. Res. 3, 249–261.

Omata, Y., Saito, Y., Fujita, K., Ogawa, Y., Nishio, K., Yoshida, Y., Niki, E., 2008. Induction of adaptive response and enhancement of PC12 cell tolerance by lipopolysaccharide primarily through the upregulation of glutathione S-transferase A3 via Nrf2 activation. Free Radic. Biol. Med. 45, 1437–1445.

Otterbein, L., Bach, F., Alam, J., Soares, M., Tao Lu, H., Wysk, M., Davis, R., Flavell, R., Choi, A., 2000. Carbon monoxide has anti-inflammatory effects involving the mitogen-activated protein kinase pathway. Nat. Med. 6, 422–428.

Reale, M., Iarlori, C., Thomas, A., Gambi, D., Perfetti, B., Di Nicola, M., Onofrj, M., 2009. Peripheral cytokines profile in Parkinson's disease. Brain Behav. Immun. 23, 55–63.

Roebuck, K., 1999. Oxidant stress regulation of IL-8 and ICAM-1 gene expression: differential activation and binding of the transcription factors AP-1 and NF-kappaB (Review). Int. J. Mol. Med. 4, 223–230.

Shibahara, S., 1988. Regulation of heme oxygenase gene expression. Semin. Hematol. 25, 370–376.

Sugama, S., 2009. Stress-induced microglial activation may facilitate the progression of neurodegenerative disorders. Med. Hypotheses 73, 1031–1034.

Syapin, P., 2008. Regulation of haeme oxygenase-1 for treatment of neuroinflammation and brain disorders. Br. J. Pharmacol. 155, 623–640.

Thimmulappa, R., Lee, H., Rangasamy, T., Reddy, S., Yamamoto, M., Kensler, T., Biswal, S., 2006. Nrf2 is a critical regulator of the innate immune response and survival during experimental sepsis. J. Clin. Invest. 116, 984–995.

Turchini, G., Quinn, G., Jones, P., Palmeri, G., Gooley, G., 2009. Traceability and discrimination among differently farmed fish: a case study on Australian Murray cod. J. Agric. Food Chem. 57, 274–281.

Vanhoecke, B., Delporte, F., Van Braeckel, E., Heyerick, A., Depypere, H., Nuytinck, M., De Keukeleire, D., Bracke, M., 2005. A safety study of oral tangeretin and xanthohumol administration to laboratory mice. In Vivo 19, 103–107.

Wilms, H., Zecca, L., Rosenstiel, P., Sievers, J., Deuschl, G., Lucius, R., 2007. Inflammation in Parkinson's diseases and other neurodegenerative diseases: cause and therapeutic implications. Curr. Pharm. Des. 13, 1925–1928.

Wu, C., Hsieh, C., Lai, P., Lin, J., Liu, Y., Wung, B., 2006. Upregulation of endothelial heme oxygenase-1 expression through the activation of the JNK pathway by sublethal concentrations of acrolein. Toxicol. Appl. Pharmacol. 214, 244–252.

Yates, M., Tran, Q., Dolan, P., Osburn, W., Shin, S., McCulloch, C., Silkworth, J., Taguchi, K., Yamamoto, M., Williams, C., Liby, K., Sporn, M., Sutter, T., Kensler, T., 2009. Genetic versus chemoprotective activation of Nrf2 signaling: overlapping yet distinct gene expression profiles between Keap1 knockout and triterpenoid-treated mice. Carcinogenesis 30, 1024–1031.

Yeh, C., Chen, T., Wang, Y., Lin, Y., Lin, P., 2009. HO-1 activation can attenuate cardiomyocytic apoptosis via inhibition of NF-kappaB and AP-1 translocation following cardiac global ischemia and reperfusion. J. Surg. Res. 155, 147–156.

Youdim, K., Qaiser, M., Begley, D., Rice-Evans, C., Abbott, N., 2004. Flavonoid permeability across an in situ model of the blood–brain barrier. Free Radic. Biol. Med. 36, 592–604.

Zanoli, P., Zavatti, M., 2008. Pharmacognostic and pharmacological profile of Humulus lupulus L. J. Ethnopharmacol. 116, 383–396.

Zhou, M., Gu, L., Zhu, N., Woods, W., Findley, H., 2003. Transfection of a dominant-negative mutant NF-kB inhibitor (IkBm) represses p53-dependent apoptosis in acute lymphoblastic leukemia cells: interaction of IkBm and p53. Oncogene 22, 8137–8144.